Temporal Self-Compression and Self-Frequency Shift of Submicrojoule Pulses at a Repetition Rate of 8 MHz

Francesco Tani,[1,*] Jacob Lampen,[2] Martin Butryn,[1] Michael H. Frosz,[1] Jie Jiang,[2] Martin E. Fermann,[2] and Philip St.J. Russell[1]

[1] *Max Planck Institute for the Science of Light, Staudtstr. 2, 91058 Erlangen, Germany*
[2] *IMRA America, Inc., 1044 Woodridge Avenue, Ann Arbor, Michigan 48105, USA*

(Received 18 August 2022; accepted 28 November 2022; published 22 December 2022)

We combine soliton dynamics in gas-filled hollow-core photonic crystal fibers with a state-of-the-art fiber laser to realize a turnkey system producing few-femtosecond pulses at 8-MHz repetition rate at pump energies as low as 220 nJ. Furthermore, by exploiting the soliton self-frequency shift in a second hydrogen-filled hollow-core fiber, we efficiently generate pulses as short as 22 fs, continuously tunable from 1100 to 1474 nm.

DOI: 10.1103/PhysRevApplied.18.064069

I. INTRODUCTION

Laser systems delivering trains of ultrashort pulses at megahertz-level repetition rates and megawatt peak powers have become key to research and applications in numerous fields [1–3]. Recent advances in laser techniques and nonlinear optics have enabled the efficient generation of pulses as short as a single cycle at average powers of tens of watts and energies from a few microjoules (μJ) up to the megajoule (MJ) level at repetition rates as high as 10 MHz [4–8]. Such remarkable specifications are typically achieved by temporally compressing about 100-fs pulses from solid-state lasers by means of hollow-core (HC) photonic crystal fibers (PCFs) and capillaries, multipass cells, and glass plates [9]. Reaching durations of a few femtoseconds (fs) requires, however, large compression ratios (∼100) and multiple stages, which is not ideal, as this results in increased system complexity and reduced throughput efficiency. Furthermore, achieving good stability is challenging at very high repetition rates, when the increased average power can cause thermal instabilities. Few-fs pulses with lower energies (a few tens of nJ up to a few hundred nJ) are typically sufficient for studying and controlling ultrafast dynamics in condensed matter systems [1–3]. Nevertheless, such pulses cannot be delivered directly by laser oscillators, and postcompression using solid-core fibers is highly inefficient and complex, requiring compensation of higher-order phase terms to reach the few-fs regime [10–12]. Moreover, most systems delivering amplified pulses with durations of a few tens of fs are centered at 0.8, 1, and 2 μm wavelengths and lack the spectral tunability that is often achieved via optical parametric amplification.

Gas-filled HC fibers provides a versatile platform both for generating few-fs pulses by temporal compression and for efficient frequency conversion [13,14]. Recent work reported exciting opportunities for using stimulated Raman scattering to efficiently generate ultrashort pulses that were wavelength-tunable in the near-infrared (IR) [15–18]. So far, however, in hollow capillaries, the large core and high loss constrain Raman-driven dynamics to the normal-dispersion regime. On the other hand, anomalous dispersion can be easily achieved in HC PCFs, permitting access to soliton dynamics such as the Raman-driven soliton self-frequency shift (SSFS), [15,16,18], which have long been studied and exploited in solid-core fibers. In comparison, the SSFS in HC PCFs allows shorter-wavelength pulses to be redshifted by an amount that can be adjusted by varying the gas pressure. Furthermore, it is possible to achieve considerably shorter pulse durations and higher pulse energies than in solid-core fibers, where the minimum pulse durations are limited to about 80 fs and the maximum energies to about 90 nJ [19–21].

Here, we report the efficient generation of 5-fs pulses (1030 nm, 8 MHz) by launching 40-fs pulses with energies in the range of 220–475 nJ, delivered from a state-of-the-art fiber laser into a gas-filled HC PCF. We then demonstrate, in a second experiment with a H_2-filled HC PCF, that the pulse wavelength can be efficiently and continuously tuned across the near-IR by the SSFS. In this fashion, we

*francesco.tani@mpl.mpg.de

generate pulses as short as 22 fs at energies between 120 and 160 nJ (∼0.95–1.28 W average power) at wavelengths from 1080 to 1474 nm. Finally, for the range of parameters considered here, both processes are highly coherent, so that carrier–envelope-phase (CEP) stability is conveniently achieved by locking the carrier–envelope-offset (CEO) frequency, f_{CEO}.

II. LASER SYSTEM AND SOLITON-EFFECT SELF-COMPRESSION

The experimental setup is shown in Fig. 1. The laser is a highly coherent 80-MHz Yb-fiber oscillator mode-locked at near-zero dispersion using a nonlinear amplifying loop mirror [22]. The system includes a down counter to 8 MHz, which permits a CEP-stable output when f_{CEO} is locked at 16 MHz. The pulse train is then amplified in a large-mode-area polarization-maintaining Yb-doped fiber (mode area 500 μm^2, length 3.0 m) by self-similar amplification [23]. In this fashion, we obtain 1030-nm about-40-fs full width at half maximum (FWHM) pulses with average powers up to 7.8 W (∼0.97-μJ pulse energy). A wire-grid polarizer is used to control the output power, followed by a half-wave plate to match the fiber-polarization axis and a planoconvex lens to couple into the HC PCF. Scanning electron micrographs (SEMs) of the two HC PCFs used in the experiments are shown in Fig. 1(b). The PCF on the left is employed for pulse compression (denoted as fiber *A* in what follows) and the second one for SSFS (denoted as fiber *B* in what follows). In both experiments, the HC PCFs are placed in gas cells with a coated fused-silica window at the input and uncoated windows at the output (a 1-mm-thick MgF_2 window after PCF *A*, and a 5-mm-thick fused-silica window after PCF *B*). The light emerging from the fibers is collimated using a silver parabolic mirror, after which the output spectra are recorded using an integrating sphere connected to a spectrum analyzer (Yokogawa) via a multimode fiber. For temporal characterization of the pulses, we use second-harmonic-generation frequency-resolved optical gating (SHG FROG) in an all-reflective noncollinear geometry, with a 10-μm-thick beta barium borate (BBO) crystal as the nonlinear medium.

Both HC PCFs have anomalous dispersion [$\beta_2(\omega_0) < 0$] at the laser frequency for Ar (and H_2) filling pressures up to several tens of bar. As a result, soliton dynamics can be conveniently accessed by launching laser pulses with peak power P_0 and duration T_0, such that the soliton order is $N = \sqrt{\gamma P_0 T_0^2/|\beta_2|} \geq 1$, where γ is the fiber nonlinear coefficient [24] and β_2 depends on the species and pressure of the gas. During propagation, higher-order solitons undergo self-compression; their duration shortens by a factor approximately proportional to N over the length $L_c = [1/(2N) + 1.7/N^2]L_D$, where L_D is the dispersion length [24]. Beyond this point, the input pulses undergo either soliton fission or a periodic evolution, depending on

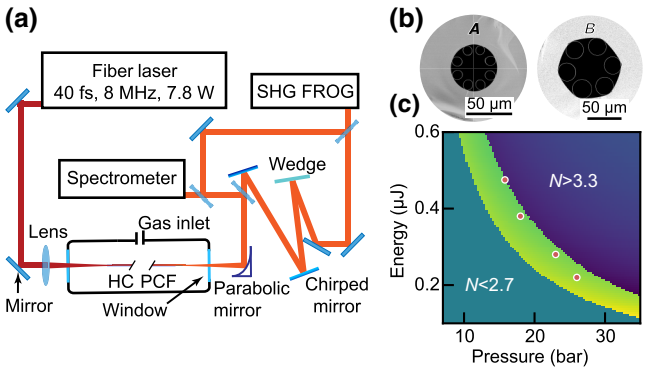

FIG. 1. (a) Sketch of the experimental setup. (b) Scanning electron micrographs of the two single-ring HC PCFs. Fiber on the left (fiber *A*) has a core diameter of 30 μm, a core-wall thickness of about 220 nm, and is used for temporal compression. Fiber on the right (fiber *B*) has a core diameter of 40 μm, a core-wall thickness of about 320 nm, and is used for SSFS. (c) Calculated compression length as a function of pulse energy and argon-filling pressure. Calculation is for a fiber filled with argon and soliton order $2.7 < N < 3.3$; light-green–yellow area marks the range of energies and pressures for which $L_C = (18 \pm 1.5)$ cm, and red dots denote experimental measurements.

the perturbations introduced by effects such as higher-order dispersion, self-steepening, and ionization. The distance L_C over which the pulses remain temporally focused (typically by a few cm) can be adjusted by varying the pressure of the filling gas, the energy of the input pulses, or adding a positive chirp. As a result, a fiber of fixed length can be employed to obtain the same compression factors over a broad range of input energies. In Fig. 1(c), we plot the range of pulse energies and Ar pressures for which about eightfold compression can be achieved in an 18-cm length of fiber *A*, which is calculated using the above expressions for N and L_c; the red dots indicate the experimental parameters. Because the FWHM of the pump laser pulses is already only a few tens of fs, we can obtain single-cycle durations at low soliton orders ($N \sim 3$), thus ensuring efficient and stable temporal compression. The plot in Fig. 1(c) shows that, by changing the gas pressure, the same fiber sample can be used to compress 40-fs pulses with energies between about 600 and 150 nJ and that much-wider energy ranges can be readily accessed using HC PCFs with different core radii and lengths.

By exploiting the scale invariance of soliton dynamics in gas-filled HC fibers [5], self-compression to a few fs is demonstrated over a wide range of pulse energies from a few μJ up to the millijoule (mJ) level [4,5,25–27]. Here, we show that the same dynamics can be reproduced using input pulses with energies as low as about 200 nJ. To demonstrate this, we use an 18-cm length of fiber *A*, in which the capillaries surrounding the core have wall thicknesses of about 220 nm, which are thin enough to avoid wavelength-dependent distortions to the dispersion

profile (caused by anticrossings between wall resonances and the core mode) and ensure high-fidelity temporal compression [28]. It is worth noting that, when HC fibers are pumped by MHz pulse trains with watt-level average power, thermal effects in the gas can affect the pulse-to-pulse stability [4,29,30]. These instabilities are caused by nonlinear absorption and ionization, which are enhanced by contamination of the filling gas by, for example, water. They can be suppressed, to a large extent, by evacuating and purging the fiber with an inert gas before the experiment and selecting the experimental parameters to minimize photoionization.

A planoconvex lens with a 10-cm focal length is used to launch the laser pulses into the HC PCF [Fig. 1(a)], resulting in an overall transmission of about 74%, in part limited by the distorted beam profile (typically >90% can be achieved in the absence of beam distortion).

Even though the few-cycle pulses at the fiber output are transform-limited, dispersion compensation is required to measure them because propagation through the gas in the cell, its output window, and in air afterwards introduces a positive chirp, which is compensated for using a pair of double-angle negatively chirped mirrors (UltraFast Innovations GmbH, group delay dispersion of -80 fs^2 per pair) in combination with thin fused-silica wedges (Altechna) for dispersion fine-tuning. Upon filling the HC PCF with Ar and tuning the pressure over the range 15.8–26 bar, we obtain similar soliton orders ($N \sim 3$) for input pulses with energies between 220 and 475 nJ, and thus, achieve comparable pulse durations at the fiber output. This is shown in Figs. 2(a) and 2(b), where we plot the retrieved temporal and spectral profiles of the compressed pulses at pump energies of 220, 280, 380, and 475 nJ. The FWHM duration is between 5.2 and 5.8 fs, with more than 76% of the energy within the main peak. The measured and retrieved FROG traces obtained after filling the fiber with 23 bar of Ar are shown in Figs. 2(c) and 2(d).

III. SOLITON SELF-FREQUENCY SHIFT IN H_2-FILLED SR PCF

To demonstrate a SSFS-based source of about 30-fs pulses with tunable central wavelength, we use 1.6 and 2.9-m lengths of fiber *B* filled with H_2. The hollow-core diameter is 40 μm, the core-wall thickness is between about 275 and 320 nm, and the fiber is coiled up in one turn with about 24-cm radius. Compared to fiber *A*, the core-wall thickness is thicker to shift the first low-loss transmission window (located at $\lambda > \lambda_{ac} = 2t\sqrt{n_{silica}^2 - n_{core}^2}$ where t is the core-wall thickness, n_{silica} is the index of silica, and n_{core} is the index of the filling gas [31,32]) to longer wavelengths to accommodate the redshifting soliton. Using a planoconvex lens with 12-cm focal length, we launch 500-nJ (corresponding to 4 W) pulses into the HC PCF and achieve about 65% transmission, which is lower than that of 74% obtained with fiber *A*, mainly because of a slightly lower coupling efficiency and higher overall loss due to the much-longer fiber length (the loss of the PCF at the pump wavelength, measured by cutback, is <0.25 dB/m). A half-wave plate is used to align the linearly polarized pump field

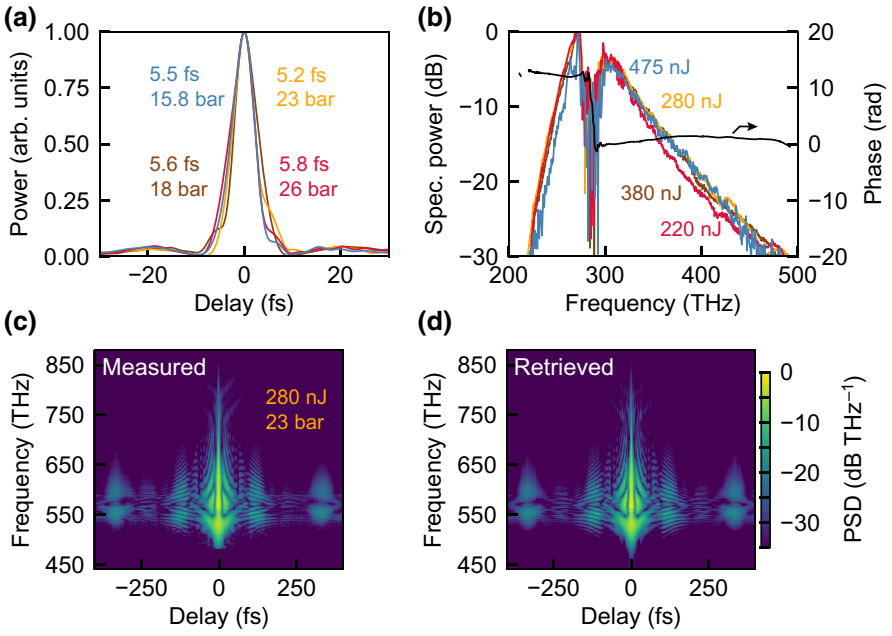

FIG. 2. (a) Temporal and (b) spectral profiles of the pulses at the output of an 18-cm length of fiber *A*. Curves are obtained from SHG FROG measurements for a selection of input pulse energies and H_2-filling pressures. Bottom panels show (c) measured and (d) retrieved FROG traces when 280-nJ pulses are launched into the fiber filled with 23 bar of H_2.

with one of the birefringent eigenaxes of the HC PCF. This is crucial for preserving the linear polarization state, which can be impaired by the long fiber length and rotational Raman nonlinearity, which can be reduced but not entirely suppressed when the pulses are shorter than the period of rotational Raman scattering (56 fs). After adjustment, the light exiting the fiber is >99% linearly polarized.

To illustrate the SSFS in H_2-filled single-ring HC PCFs, Figs. 3(a) and 3(b) show the simulated temporal and spectral pulse evolution in fiber *B* filled with 40-bar H_2. A unidirectional nonlinear wave equation [33], with the Raman polarization term represented by a response function, is used in the modeling, as discussed in Ref. [34]. The optical loss is included using the empirical formula given in Ref. [32], and as the input we use the pulse parameters measured by the SHG FROG at an energy of 220 nJ (soliton order ∼2.6). Under these conditions, photoionization of the gas, calculated using the Perelomov-Popov-Terent'ev (PPT) rate, modified with the Ammosov-Delone-Krainov (ADK) coefficients [35], is negligible, i.e., the free-electron density is close to zero.

For a fixed set of gas and laser parameters, the redshift increases with fiber length, but ultimately it is limited by the waveguide loss and absorption in H_2. The pump pulse first undergoes soliton-effect self-compression and then, after about 40 cm of propagation, a redshifting soliton emerges, shifting to longer wavelength, reaching 1385 nm after 1.6 m and 1480 nm after 2.9 m. At this last position, about 18.7% of the input pulse energy is absorbed by H_2 and the redshifted soliton carries about 53% of the output power. Apart from fiber loss and H_2 absorption, the fraction of input energy carried by the redshifted component is affected by the soliton order, *N*, with higher values resulting in a less-redshifted fraction. According to simulations, this fraction varies between 87% and 53% when the pressure is varied from 5 to 40 bar, corresponding to soliton orders between about 1.0 and 3.7. The simulated and measured spectra are in excellent agreement. In Fig. 3(c), we show the spectra measured at the output of the fiber filled with H_2 in the same pressure range and compare the measured and simulated spectra in PCFs with lengths of 1.6 m [Fig. 3(d)] and 2.9 m [Fig. 3(e)], filled with 40-bar H_2. For the selected experimental parameters, the wavelength can be continuously tuned between 1080 and 1474 nm, while the redshifted solitons carry over 0.95 W of average power (∼120 nJ) and up to 1.28 W (∼160 nJ) at 1300 nm. We also find that a lower pulse energy (by ∼30%) is needed in the simulations to reproduce the measured spectra, in agreement with the experimental observations that, compared to theory, a larger fraction of energy is lost during propagation, resulting in a slightly lower conversion efficiency to the redshifted peak. We attribute this to excitation of higher-order modes at the fiber input, which causes the appearance of a tall and narrow spectral peak around 1030 nm that is not reproduced in numerical simulations. Using a 10-nm-wide bandpass filter to isolate this spectral region, we are able to confirm that at this wavelength the light is indeed in a higher-order mode (HOM) and carries about 15% of the output power. The radiation in the rest of the spectrum is in a pure fundamental mode. This observation may explain the discrepancy between simulations and experiments, since optical loss is much higher for HOMs.

This LP02-like HOM does not undergo any spectral broadening nor does it affect the SSFS. Due to its different group velocity, in fact, it walks off quickly from the

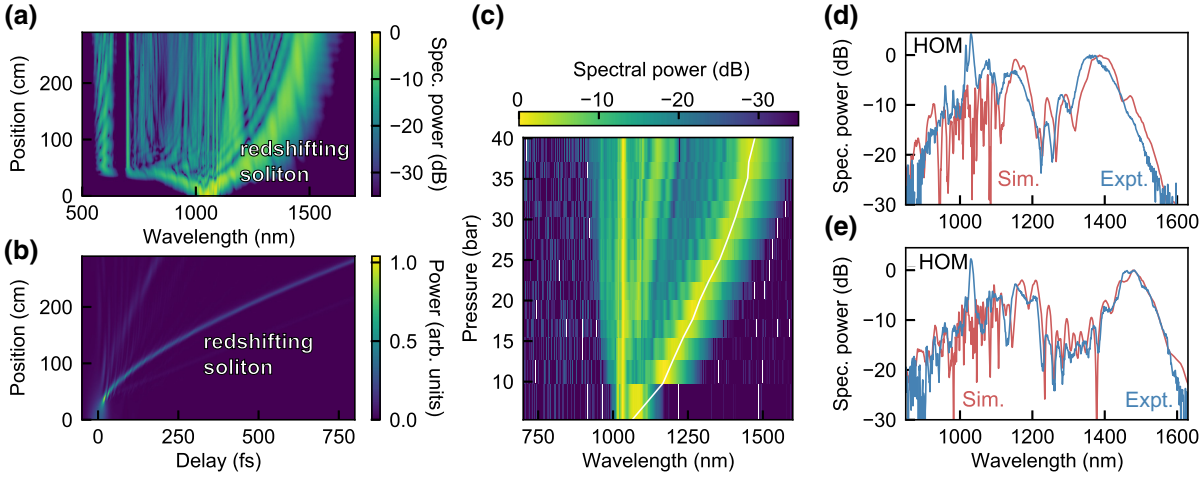

FIG. 3. Simulated (a) spectral and (b) temporal evolution of a 220-nJ pulse in fiber *B* filled with 40 bar of H_2. (c) Measured spectra at the fiber output as a function of the H_2-filling pressure with the white line indicating the average wavelength of the redshifted soliton. (d) Measured (blue) and simulated (red) spectra for a 1.6-m length of fiber filled with 40 bar of H_2. (e) Same as (d) but using a 2.9-m-long fiber. Spectra are normalized to the peak of the redshifted spectral components. As input pulses for the numerical simulations, we use the measured temporal profile with an energy of 220 nJ.

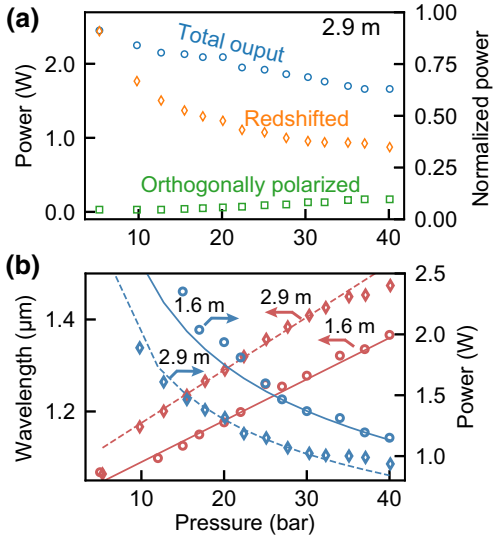

FIG. 4. (a) Power recorded as a function of H_2-filling pressure in a 2.9-m length of fiber *B*. Blue dots mark the total output power, orange diamonds the power carried by the redshifted spectral component, and green squares the output power of light polarized orthogonally to the input polarization axis. Right-hand axis indicates the power normalized to the total output power when the fiber is filled with 1 bar of H_2. (b) Central wavelength (red symbols) and power (blue symbols) of the redshifted solitons in 1.6-m (circles) and 2.9-m (diamonds) lengths of fiber *B*. In both panels, full curves are meant as guides to the eye. Blue lines denote fits of data to A/N, where $A = 3.5$ for the solid line and $A = 2.6$ for the dashed line. Red lines are linear fits of the wavelengths as a function of pressure.

main pulse. Moreover, the larger negative dispersion of the HOM results in $N < 1$, thus preventing any soliton dynamics. We attribute excitation of the HOM to transverse variations in refractive index caused by the absorption of light in H_2 [30]. The narrow bandwidth of the HOM signal suggests that it is excited close to the fiber input; if it were generated further along the fiber by intermodal four-wave mixing, a larger bandwidth would be expected, since the pump pulse will undergo spectral broadening. In contrast with the Ar-filled fiber, when no HOM is observed at the output, a HOM appears every time in the H_2-filled PCF in a narrow spectral region around 1030 nm, despite careful alignment. Measurements of the laser power after the fiber [Fig. 4(a)] further support the hypothesis. The total output and red-spectral-component power both decrease steadily as the H_2-filling pressure goes up. The waveguide loss, which is higher at longer wavelength, gas absorption, and higher soliton order (which increases with pressure) only partially explain this behavior. At the same time, the degree of polarization degrades at higher pressure, and at 40 bar about 10% of the output power is polarized orthogonally to the redshifted soliton, which is still linearly polarized and in the fundamental mode. In Fig. 4(b), we show the average wavelength and power of the redshifted spectral component after lengths of 1.6 and 2.9 m. The power is obtained from calibrated spectral measurements and further confirmed by using long-pass filters followed by a thermal power meter. In the shorter PCF, the power of the red spectral component at a selected wavelength is up to 10% higher, but the maximum redshift is limited to 1370 nm (1474 nm for the longer fiber). Like in solid-core fibers, where the redshift is proportional to the nonlinear coefficient, γ [24], here, the redshift is approximately linear with gas pressure (like γ). Except for an offset due to optical loss, for both fiber lengths, the power in the redshifted component is approximately inversely proportional to the soliton order, *N*. This is because the redshifting soliton emerges after the pulse undergoes soliton-effect self-compression, and the fraction of power carried by the

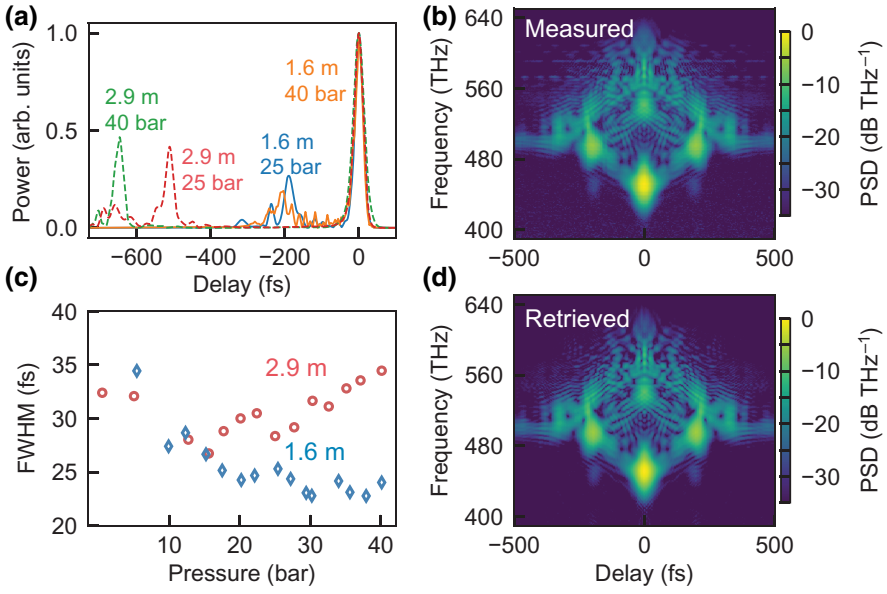

FIG. 5. (a) Measured temporal pulse profile after the 1.6-m-long PCF (solid lines) and the 2.9-m-long PCF (dashed lines) at 25 and 40 bar of H_2. (c) Measured FWHM pulse duration at the output of the two fibers as a function of pressure. (b) Measured and (d) retrieved FROG traces at the output of the 1.6-m-long PCF filled with 30 bar of H_2.

shortened pulse is determined by the quality factor, which is approximately $1/N$.

A SHG FROG is used for temporal characterization of the output pulses and is placed directly after the parabolic mirror used for recollimation and an achromatic half-wave plate. The dispersion introduced by the optical components (between –20 and +10 fs^2/mm in the spectral region 1100–1500 nm, affecting the pulse duration by only a few fs) is accounted for in data postprocessing. The retrieved FROG traces reveal redshifted pulses with a clean Gaussian-like temporal profile [Fig. 5(a)] and FWHM durations as short as 22 fs. These pulses arrive a few hundreds of fs after the higher frequencies, a delay that increases with gas pressure and fiber length. Figure 5(b) shows the measured FWHM duration of the redshifted pulses as a function of pressure for the two fiber lengths. In the 1.6-m-long PCF, the redshifted pulses shorten with increasing H_2 pressure, stabilizing at (24 ± 1.5) fs above 20 bar. For the 2.9-m-long PCF, on the other hand, the redshifted pulse duration reaches a minimum (∼27 fs) when filled with 15-bar H_2, slowly increasing for higher pressures and reaching 34 fs at 40 bar. By reducing the power and frequency downshift, optical loss also affects the soliton dynamics, and thus, the duration of the redshifted pulses. Because the pulse energy falls with propagation along the fiber, N eventually becomes less than one, when the redshifting pulse stops being a soliton and acquires a chirp.

IV. CONCLUSIONS

Soliton self-compression in gas-filled HC PCFs, combined with a state-of-the-art fiber laser delivering 40-fs pulses with energies in the few 100 s of nJ range and at a repetition rate of 8 MHz, results in a simple, efficient, and stable source of 5-fs pulses. By exploiting the soliton self-frequency shift in hydrogen-filled HC PCFs, pulses as short as 22 fs, with energies in the range of 120–160 nJ (average power up to 1.28 W) can be generated at wavelengths continuously tunable between about 1100 and 1500 nm. This spectral region is important for multiphoton imaging of biological samples. These pulses have much higher energy and several-times-shorter durations than those previously achieved using SSFS in waveguides [18–21]. The conversion efficiency to the redshifted pulses varies between about 30% and 50% and is limited by optical loss (mostly absorption by H_2), incoupling losses, and excitation of the higher-order mode through thermal effects. The efficiency can be further increased by optimizing the launch efficiency (currently $>70\%$) and using a pressure gradient to lower the pressure at the fiber input, thus mitigating thermal effects in the gas and further increasing the energy in the redshifted solitons.

[1] M. Garg and K. Kern, Attosecond coherent manipulation of electrons in tunneling microscopy, Science **367**, 411 (2020).

[2] C. Heide, M. Hauck, T. Higuchi, J. Ristein, L. Ley, H. B. Weber, and P. Hommelhoff, Attosecond-fast internal photoemission, Nat. Photonics **14**, 4 (2020).

[3] M. Plankl, P. E. Faria Junior, F. Mooshammer, T. Mooshammer, M. Zizlsperger, F. Sandner, F. Schiegl, S. Maier, M. A. Huber, M. Gmitra, *et al.*, Subcycle contact-free nanoscopy of ultrafast interlayer transport in atomically thin heterostructures, Nat. Photonics **15**, 594 (2021).

[4] F. Köttig, D. Schade, J. R. Koehler, P. St.J. Russell, and F. Tani, Efficient single-cycle pulse compression of an ytterbium fiber laser at 10 MHz repetition rate, Opt. Express **28**, 9099 (2020).

[5] D. Schade, F. Köttig, J. R. Koehler, M. H. Frosz, P. St.J. Russell, and F. Tani, Scaling rules for high quality soliton self-compression in hollow-core fibers, Opt. Express **29**, 19147 (2021).

[6] C.-H. Lu, T. Witting, A. Husakou, M. J. J. Vrakking, A. H. Kung, and F. J. Furch, Sub-4 fs laser pulses at high average power and high repetition rate from an all-solid-state setup, Opt. Express **26**, 8941 (2018).

[7] M. Müller, J. Buldt, H. Stark, C. Grebing, and J. Limpert, Multipass cell for high-power few-cycle compression, Opt. Lett. **46**, 2678 (2021).

[8] S. Hädrich, M. Kienel, M. Müller, A. Klenke, R. Rothhardt, R. Klas, T. Gottschall, T. Eidam, A. Drozdy, P. Jójárt, *et al.*, Energetic sub-2-cycle laser with 216 W average power, Opt. Lett. **41**, 4332 (2016).

[9] T. Nagy, P. Simon, and L. Veisz, High-energy few-cycle pulses: Post-compression techniques, Adv. Phys. X **6**, 1845795 (2021).

[10] A. A. Amorim, M. V. Tognetti, P. Oliveira, J. L. Silva, L. M. Bernardo, F. X. Kärtner, and H. M. Crespo, Sub-two-cycle pulses by soliton self-compression in highly nonlinear photonic crystal fibers, Opt. Lett. **34**, 3851 (2009).

[11] A. M. Heidt, J. Rothhardt, A. Hartung, H. Bartelt, E. G. Rohwer, J. Limpert, and A. Tünnermann, High quality sub-two cycle pulses from compression of supercontinuum generated in all-normal dispersion photonic crystal fiber, Opt. Express **19**, 13873 (2011).

[12] P. Dienstbier, F. Tani, T. Higuchi, J. Travers, P. St.J. Russell, and P. Hommelhoff, Generation of 15 cycle pulses at 780 nm at oscillator repetition rates with stable carrier-envelope phase, Opt. Express **27**, 24105 (2019).

[13] C. Markos, J. C. Travers, A. Abdolvand, B. J. Eggleton, and O. Bang, Hybrid photonic-crystal fiber, Rev. Mod. Phys. **89**, 045003 (2017).

[14] P. St.J. Russell, P. Hölzer, W. Chang, A. Abdolvand, and J. C. Travers, Hollow-core photonic crystal fibres for gas-based nonlinear optics, Nat. Photonics **8**, 278 (2014).

[15] P. A. Carpeggiani, G. Coccia, F. Fan, E. Kaksis, A. Pugžlys, A. Baltuška, R. Piccoli, Y.-G. Jeong, A. Rovere, R. Morandotti, *et al.*, Extreme Raman red shift: Ultrafast multimode nonlinear space-time dynamics, pulse compression, and broadly tunable frequency conversion, Optica **7**, 1349 (2020).

[16] R. Safaei, G. Fan, O. Kwon, K. Légaré, P. Lassonde, B. E. Schmidt, H. Ibrahim, and F. Légaré, High-energy

multidimensional solitary states in hollow-core fibres, Nat. Photonics **14**, 12 (2020).

[17] S. Loranger, P. St.J. Russell, and D. Novoa, Sub-40 fs pulses at 1.8 μm and MHz repetition rates by chirp-assisted Raman scattering in hydrogen-filled hollow-core fiber, J. Opt. Soc. Am. B **37**, 3550 (2020).

[18] Y.-H. Chen, P. Sidorenko, E. Antonio-Lopez, R. Amezcua-Correa, and F. Wise, Efficient soliton self-frequency shift in hydrogen-filled hollow-core fiber, Opt. Lett. **47**, 285 (2022).

[19] H. Delahaye, C.-H. Hage, S. M. Bardet, I. Tiliouine, G. Granger, D. Gaponov, L. Lavoute, M. Jossent, S. Aleshkina, M. Salganskii, *et al.*, Generation of megawatt soliton at 1680 nm in very large mode area antiresonant fiber and application to three-photon microscopy, J. Opt. **23**, 115504 (2021).

[20] K. Wang and C. Xu, Tunable high-energy soliton pulse generation from a large-mode-area fiber and its application to third harmonic generation microscopy, Appl. Phys. Lett. **99**, 071112 (2011).

[21] L. Rishøj, B. Tai, P. Kristensen, and S. Ramachandran, Soliton self-mode conversion: Revisiting Raman scattering of ultrashort pulses, Optica **6**, 304 (2019).

[22] M. E. Fermann, F. Haberl, M. Hofer, and H. Hochreiter, Nonlinear amplifying loop mirror, Opt. Lett. **15**, 752 (1990).

[23] M. E. Fermann, V. I. Kruglov, B. C. Thomsen, J. M. Dudley, and J. D. Harvey, Self-Similar Propagation and Amplification of Parabolic Pulses in Optical Fibers, Phys. Rev. Lett. **84**, 6010 (2000).

[24] G. P. Agrawal, *Nonlinear Fiber Optics* (Academic Press, Amsterdam, 2007).

[25] F. Emaury, C. F. Dutin, C. J. Saraceno, M. Trant, O. H. Heckl, Y. Y. Wang, C. Schriber, F. Gerome, T. Südmeyer, F. Benabid, *et al.*, Beam delivery and pulse compression to sub-50 fs of a modelocked thin-disk laser in a gas-filled kagome-type HC-PCF fiber, Opt. Express **21**, 4986 (2013).

[26] K. F. Mak, M. Seidel, O. Pronin, M. H. Frosz, A. Abdolvand, V. Pervak, A. Apolonski, F. Krausz, J. C. Travers, and P. St.J. Russell, Compressing μJ-level pulses from 250 fs to Sub-10 fs at 38-MHz repetition rate using two gas-filled hollow-core photonic crystal fiber stages, Opt. Lett. **40**, 1238 (2015).

[27] J. C. Travers, T. F. Grigorova, C. Brahms, and F. Belli, High-energy pulse self-compression and ultraviolet generation through soliton dynamics in hollow capillary fibres, Nat. Photonics **13**, 8 (2019).

[28] F. Tani, F. Köttig, D. Novoa, R. Keding, and P. St.J. Russell, Effect of anti-crossings with cladding resonances on ultrafast nonlinear dynamics in gas-filled photonic crystal fibers, Photonics Res. **6**, 84 (2018).

[29] J. R. Koehler, F. Köttig, B. M. Trabold, F. Tani, and P. St.J. Russell, Long-Lived Refractive-Index Changes Induced by Femtosecond Ionization in Gas-Filled Single-Ring Photonic-Crystal Fibers, Phys. Rev. Appl. **10**, 064020 (2018).

[30] J. R. Koehler, F. Köttig, D. Schade, P. St.J. Russell, and F. Tani, Post-recombination effects in confined gases photoionized at megahertz repetition rates, Opt. Express **29**, 4842 (2021).

[31] J.-L. Archambault, R. J. Black, S. Lacroix, and J. Bures, Loss calculations for antiresonant waveguides, J. Lightwave Technol. **11**, 416 (1993).

[32] L. Vincetti and L. Rosa, A simple analytical model for confinement loss estimation in hollow-core tube lattice fibers, Opt. Express **27**, 5230 (2019).

[33] F. Tani, J. C. Travers, and P. St.J. Russell, Multimode ultrafast nonlinear optics in optical waveguides: Numerical modeling and experiments in kagomé photonic-crystal fiber, J. Opt. Soc. Am. B **31**, 311 (2014).

[34] J. K. Wahlstrand, S. Zahedpour, Y.-H. Cheng, J. P. Palastro, and H. M. Milchberg, Absolute measurement of the ultrafast nonlinear electronic and rovibrational response in H_2 and D_2, Phys. Rev. A **92**, 063828 (2015).

[35] A. Couairon and A. Mysyrowicz, Femtosecond filamentation in transparent media, Phys. Rep. **441**, 47 (2007).